ANL/MSD/CP-103004

MICROSTRUCTURE AND ELECTRICAL PROPERTIES OF EPITAXIAL $SrBi_2Nb_2O_9$ and $SrBi_2Ta_2O_9$ FILMS*

M.A. Zurbuchen[1], J. Lettieri[1], S. K. Streiffer[2], Y. Jia,[1] M. E. Hawley[3], X. Pan[4], A. H. Carim[1], and D. G. Schlom[1],

[1]Department of Materials Science and Engineering
The Pennsylvania State University
University Park, PA 16802-5005

[2]Materials Science Division
Argonne National Laboratory
Argonne, IL 60439

[3]Materials Science and Technology Division
Los Alamos National Laboratory
Los Alamos, NM 87545

[4]Dept. of Mater. Sci. & Engr.
University of Michigan
Ann Arbor, MI 48109-2136

September 2000

Paper to be presented at the Integrated Ferroelectric Meeting, Aachen, Germany, held on March 12-15, 2000.

*We wish to acknowledge support from the U. S. Department of Energy through grant DE-FG02-97ER45638 and BES-Materials Sciences, under Contract W-31-109-ENG-38.

DISCLAIMER

Portions of this document may be illegible in electronic image products. Images are produced from the best available original document.

MICROSTRUCTURE AND ELECTRICAL PROPERTIES OF EPITAXIAL $SrBi_2Nb_2O_9$ AND $SrBi_2Ta_2O_9$ FILMS

MARK A. ZURBUCHEN,[a,b] JAMES LETTIERI,[a] STEPHEN K. STREIFFER,[c] YUNFA JIA,[a,d] MARILYN E. HAWLEY,[e] XIAOQING PAN,[f] ALTAF H. CARIM,[a] and DARRELL G. SCHLOM[a,b]
[a] Department of Materials Science and Engineering, The Pennsylvania State University, University Park, PA 16803-6002, U.S.A.; [b] On leave at the Institute of Physics, Augsburg University, D-86159 Augsburg, Germany; [c] Materials Science Division, Argonne National Laboratory, Argonne, IL 60439, U.S.A; [d] On leave from Qingdao University, People's Republic of China; [e] Materials Science and Technology Division, Los Alamos National Laboratory, Los Alamos, NM 87545, U.S.A; [f] Department of Materials Science and Engineering, University of Michigan, Ann Arbor, MI 48109-2136, U.S.A.

$SrBi_2Nb_2O_9$ (and in some cases $SrBi_2Ta_2O_9$) epitaxial thin films were deposited on (001), (110), and (111) $SrTiO_3$ substrates by pulsed laser deposition (PLD), both with and without epitaxial $SrRuO_3$ bottom electrodes. Films grow epitaxially with the *c*–axis inclined by 0°, 45°, and 57° from the substrate surface normal, respectively. Greater tilts of the *c*–axis into the plane of the substrate surface provide a greater component of the polar axis (the *a*–axis of the orthorhombic unit cell) perpendicular to the substrate surface, leading to increased remanent polarization (P_r) values. Portions of the same films used for electrical characterization were examined by transmission electron microscopy (TEM). Films have a single *c*–axis tilt angle and are fully crystalline with no observable second-phase inclusions. All films are observed to have a high density of out–of–phase boundaries (OPBs).

KEYWORDS transmission electron microscopy (TEM); epitaxial growth; $SrBi_2Nb_2O_9$; $SrBi_2Ta_2O_9$; out-of-phase boundaries (OPBs); microstructure of $SrBi_2Nb_2O_9$ and $SrBi_2Ta_2O_9$

INTRODUCTION

Although there is considerable interest in thin films of the Aurivillius phase ferroelectrics $SrBi_2Nb_2O_9$ and $SrBi_2Ta_2O_9$ for use in ferroelectric memories,[1] interest in oriented or epitaxial films of these materials for such an application has been low. This is primarily because epitaxial films deposited on {001} perovskite subcell surfaces of the most commonly-used perovskite substrates, i.e., $SrTiO_3$, $LaAlO_3$, $NdGaO_3$, and $LaAlO_3$–Sr_2AlTaO_6 (LSAT), grow with their *c*–axis normal to the surface.[2,3] Such an orientation renders the material useless for ferroelectric memories, for the reason described below. However, oriented films offer the possibility of achieving films with greater remanent polarization (P_r) than is possible in randomly-oriented films.

The room temperature structures of $SrBi_2Nb_2O_9$ and $SrBi_2Ta_2O_9$ belong to the space group $A2_1am$.[4,5] That is, a mirror plane lies perpendicular to the *c*–axis, and a glide plane lies perpendicular to the *b*–axis. Both of these operations involve reflection, so from Neumann's Law, no remanent polarization can exist along either the *b*–axis or the *c*–axis. Therefore, the polar axis in orthorhombic $SrBi_2Nb_2O_9$ (and isostructural $SrBi_2Ta_2O_9$) lies entirely along the *a*–axis.[6] When the *c*–axis is perpendicular to the substrate surface (a *c*–axis film), the *a*–axis lies in the plane of the substrate, perpendicular to the applied electric field of the traditional high-density capacitor geometry relevant to ferroelectric memories. Thus, no remanent polarization exists in *c*–axis films.

In order to produce films with a ferroelectric response perpendicular to the film surface (i.e., for devices), it is necessary to grow films with some component of the polar axis (the *a*–axis) out of plane. Polycrystalline films grown by various techniques exhibit P_r values ranging from about 3.0 to 12.5 □C/cm^2.[7] However, randomly-oriented films are limited to a maximum P_r of $P_s/2$,[8] where P_s is the magnitude of the spontaneous polarization vector. In order to achieve higher P_r values, $SrBi_2Nb_2O_9$ and $SrBi_2Ta_2O_9$ films must be oriented with a greater portion of the polar axis perpendicular to the surface plane.

One route of achieving this goal is through epitaxy. $SrBi_2Ta_2O_9$ has been grown on (100) $LaSrAlO_4$, with the *c*–axis in the plane of the substrate surface,[3] providing a $1/\sqrt{2}$ component of the spontaneous polarization vector out of plane. Unfortunately, attempts to grow this orientation with a bottom electrode[9] have been unsuccessful. A way in which we have been able to tilt the *c*–axis away from the substrate surface normal *and* to incorporate a bottom electrode is by growing $SrBi_2Ta_2O_9$ and $SrBi_2Nb_2O_9$ on non–{001} perovskite substrates.[10,11]

MORPHOLOGY..EPITAXIAL $SrBi_2Nb_2O_9$..FILMS

We have grown $SrBi_2Nb_2O_9$ (and in some cases $SrBi_2Ta_2O_9$) by pulsed laser deposition (PLD) on three types of $SrTiO_3$ substrates: (001), (110), and (111), both with and without an epitaxial $SrRuO_3$ bottom electrode. Complete growth conditions,[2,3,10-12] electrical measurement results,[10,11] atomic force microscopy (AFM) analysis,[2,8,12,13] 4–circle x–ray diffraction plots,[2,3,8,10,11] and transmission electron microscopy (TEM) characterization[2,8,10,11,13,14] are presented elsewhere. We present here an overview of our results, with an emphasis on TEM investigations of all three film orientations, describing microstructural features of potential significance to ferroelectric memory devices.

ORIENTATION RELATIONSHIPS

$SrBi_2Nb_2O_9$ and $SrBi_2Ta_2O_9$ grow epitaxially on a (001) $SrTiO_3$ surface with the *c*–axis parallel to the substrate surface normal, as shown in Fig. 1. The spontaneous polarization vector in this film orientation lies entirely in the plane of the substrate surface, so no remanent polarization is measured perpendicular to this type of film.[15]

$SrBi_2Nb_2O_9$ grows epitaxially on (110) $SrTiO_3$ with the *c*–axes of twins tilted ±45° from surface normal and with an irrational plane, the (1 1 6.44) plane, which is tilted 2.03° from (116), of the ferroelectric parallel to the surface. This orientation relationship is schematically shown in Fig. 1. The equivalent tilts of the *a* and *b*–axes with respect to an electric field applied perpendicular to the film allows us to calculate a lower bound for P_s from the P_r of the film.[11] Because of the special geometry of this orientation, this result is independent of *a*/*b* twinning and is independent of whether domain switching in $SrBi_2Nb_2O_9$ is limited to 180° domain switching or also occurs via 90° domain switching (i.e., via the interchange of the *a* and *b*–axes).

$SrBi_2Nb_2O_9$ films deposited on (111) $SrTiO_3$ surfaces grow with a three-fold, 120° twin structure, with the $SrBi_2Nb_2O_9$ (103) plane parallel to the substrate surface. This orientation relationship is schematically shown in Fig. 1. The *c*–axes of the twins are tilted 57° from substrate surface normal, bringing a large component of the *a*–axis (the polar axis) out of the surface plane.

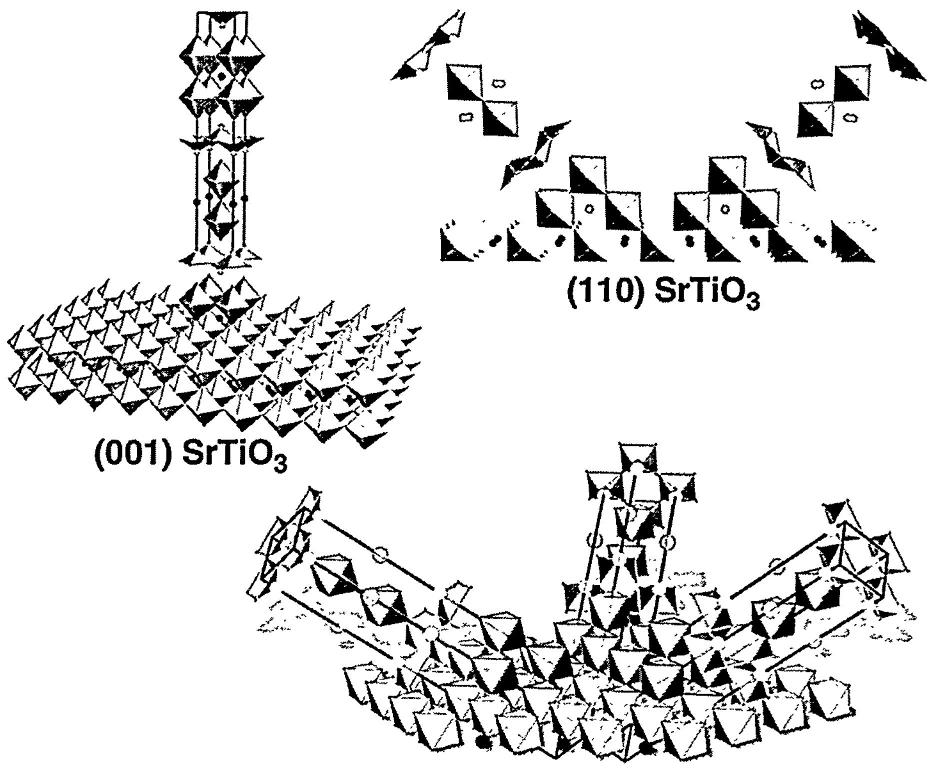

FIGURE 1 $SrBi_2Nb_2O_9$ and $SrBi_2Ta_2O_9$ grow epitaxially on (001) $SrTiO_3$ with the *c*–axis parallel to the substrate surface normal, on (110) $SrTiO_3$ in a two-fold twin structure with the *c*–axes tilted by ±45° from the surface normal, and on (111) $SrTiO_3$ in a 3–fold twin structure with the *c*–axes tilted by 57° away from surface normal.

MICROSTRUCTURE OF FILMS GROWN ON (001) $SrTiO_3$

While *c*–axis films grown on {001} perovskite substrates are not useful for ferroelectric memory devices,[15] their untwinned structure and simple orientation geometry makes them useful for investigating the microstructure of $SrBi_2Nb_2O_9$ and $SrBi_2Ta_2O_9$ films deposited by PLD under the same conditions as the films grown on (110) and (111) $SrTiO_3$ substrates.

The films are untwinned (ignoring *a–b* twinning), and no evidence of second-phase inclusions can be found. A single early sample showed evidence of an 80 Å-thick epitaxial β–Bi_2O_3 layer at the interface,[14] but subsequent adjustment of the deposition parameters, allowing the extra Bi to boil off, resulted in films free of this layer. Figure 2 shows a cross-sectional

TEM image of a typical region of $SrBi_2Ta_2O_9$; $SrBi_2Nb_2O_9$ films exhibit a similar structure. Dark, wavy bands of contrast are out-of-phase boundaries (OPBs), consisting of an offset of a fraction of the unit cell *c*–dimension between the two regions of the grain on either side of the OPB.

FIGURE 2 Cross-sectional high-resolution TEM image of (001) $SrBi_2Ta_2O_9$ / (001) $SrTiO_3$ viewed along the $[100]_{SrTiO_3}$ zone axis. Dark, undulating bands of contrast are out–of–phase boundaries (OPBs).

We observe OPBs in all of our $SrBi_2Nb_2O_9$ and $SrBi_2Ta_2O_9$ films examined by TEM. High-resolution TEM images of two OPBs are shown in Fig. 3. The OPB in Fig. 3(a) is viewed nearly edge-on. Bright spots corresponding to the bismuth oxide double layers are continuous across the grain, aside from the offset of the OPB. The OPB in Fig. 3(b) is tilted with respect to the viewing direction, so it appears wide in this image.

TEM observation indicates that multiple mechanisms contribute to the nucleation of these defects. One mechanism is shown in Fig. 4. As two $SrBi_2Nb_2O_9$ nuclei nucleated on different terraces of a $SrTiO_3$ substrate meet, their misregistry will result in an OPB. A full analysis of OPB nucleation mechanisms can be found elsewhere.[13]

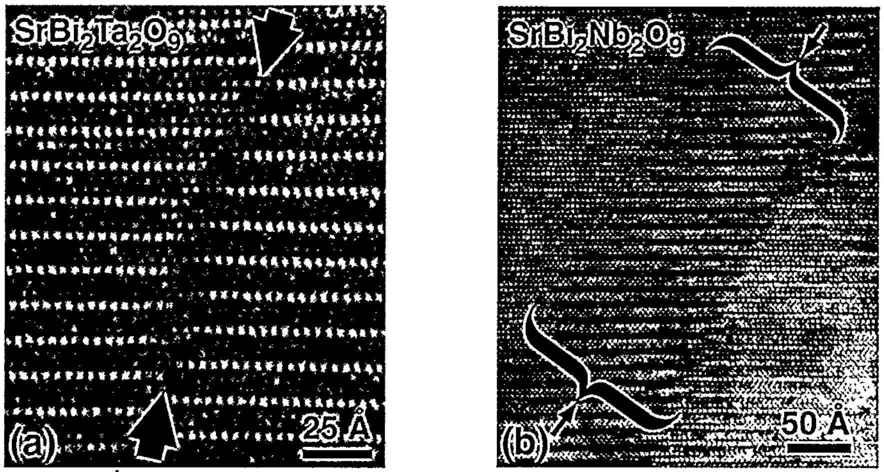

FIGURE 3 High-resolution TEM images along the $[100]_{SrTiO_3}$ zone axis of OPBs in *c*–axis oriented films. (a) an OPB viewed edge-on in $SrBi_2Ta_2O_9$ / (001) $SrTiO_3$ and (b) an OPB tilted with respect to the viewing direction in $SrBi_2Nb_2O_9$ / (001) $SrTiO_3$.

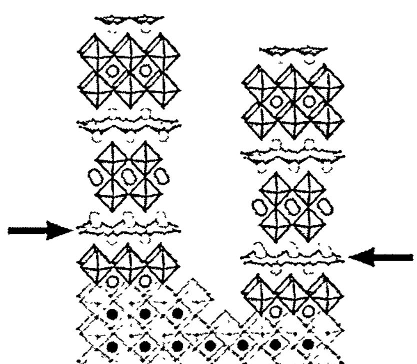

FIGURE 4 Schematic of one of the formation mechanisms of OPBs in $SrBi_2Nb_2O_9$ as two nuclei formed on opposite sides of a unit cell step on a (001) perovskite surface coalesce. The arrows mark the positions of the Bi_2O_2 layers which are vertically offset from each other by the lattice parameter of the substrate.

MICROSTRUCTURE OF FILMS GROWN ON (110) $SrTiO_3$

A cross-sectional high-resolution TEM image of a $SrBi_2Nb_2O_9$ film grown on (110) $SrTiO_3$ with an epitaxial $SrRuO_3$ bottom electrode is shown in Fig. 5. The electrode surface exhibits some roughness due to faceting at the $SrBi_2Nb_2O_9$ growth temperature (~880 °C). The film has a peak-to-valley surface roughness of 65 nm, ~20% of the full film thickness. Along this viewing direction, $[001]_{SrTiO_3}$, the columnar grains range from 50 to 800 nm in width, although it is important to keep in mind the anisotropy of the twin structure. Corroboration of this data with AFM data and other TEM views allows a full description of the three-dimensional grain structure.[13]

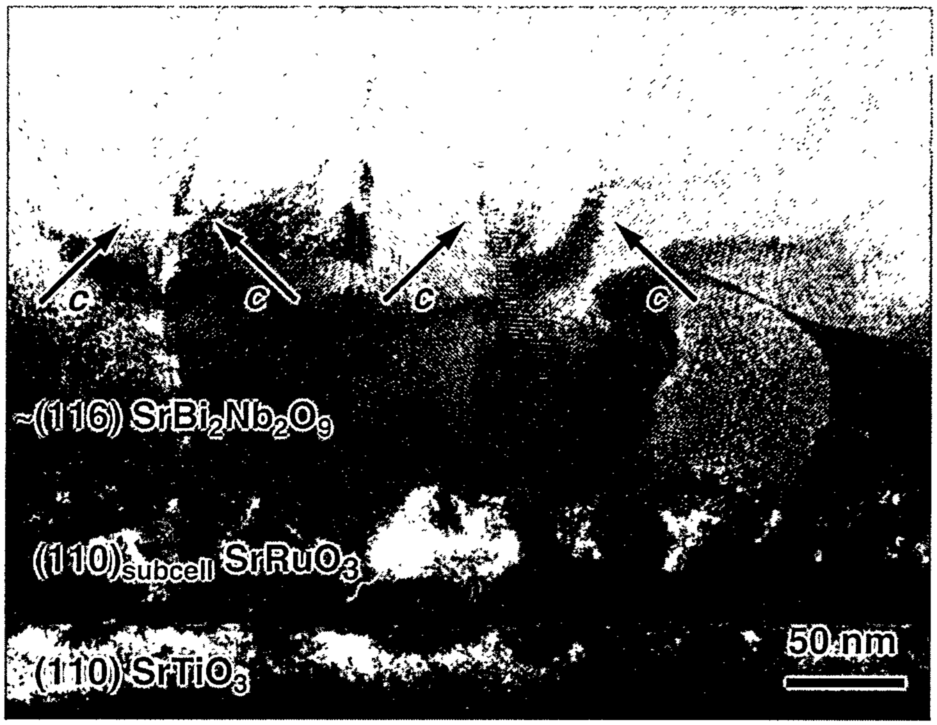

FIGURE 5 Cross-sectional high-resolution TEM image of a piece of the same ~(116) $SrBi_2Nb_2O_9$ / $(110)_{subcell}$ $SrRuO_3$ / (110) $SrTiO_3$ sample used for electrical characterization, viewed along the $[001]_{SrTiO_3}$ zone axis. The ±45° tilted *c*–axis twin structure is apparent. Arrows indicate the direction of the *c*–axes in the twins.

OPBs in $SrBi_2Nb_2O_9$ grown on (110) $SrTiO_3$ have the same type of structure as the OPBs in $SrBi_2Nb_2O_9$ grown on (001) $SrTiO_3$, but due to the *c*–axis tilt tend to penetrate the full thickness of the film. A close-up of a single OPB is shown in Fig. 6(a), showing the similar morphology. All interfaces and twin boundaries in the films are atomically clean; two are shown in Figs. 6(b) and 6(c). The P_r of the film shown in Figs. 5 and 6 is 11.4 □C/cm^2.[11] From this, we can calculate P_s to be at least 22.8 □C/cm^2.[11]

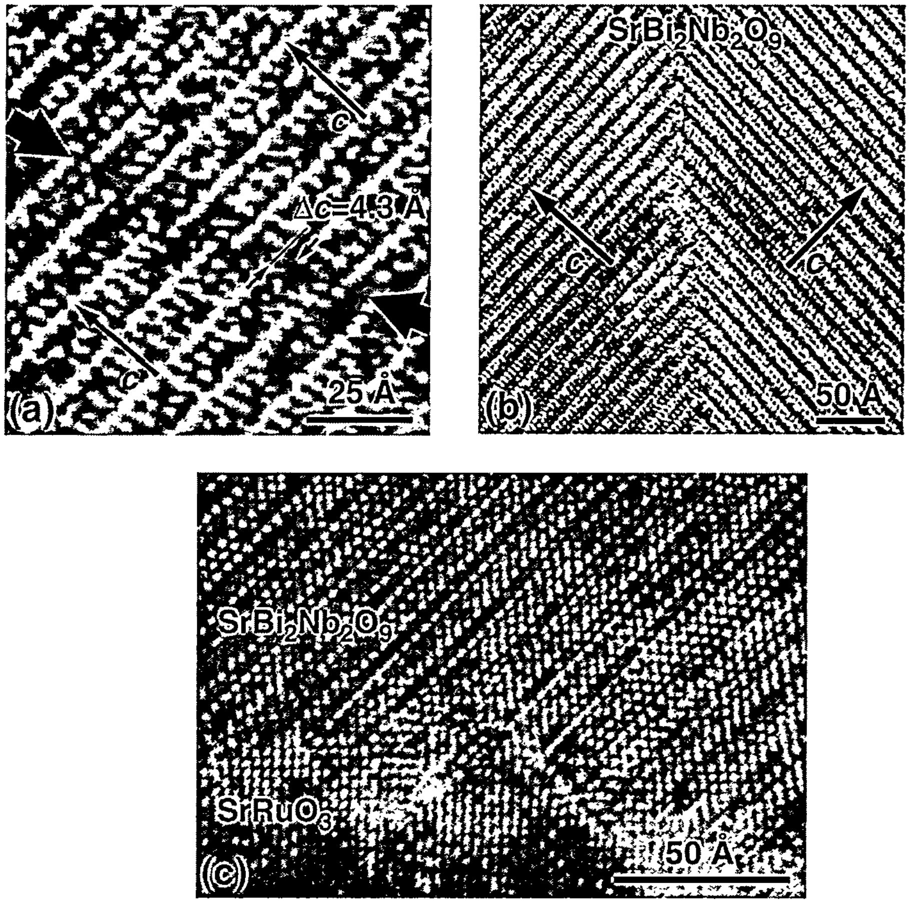

FIGURE 6 Cross-sectional high-resolution TEM images of ~(116) $SrBi_2Nb_2O_9$ / $(110)_{subcell}$ $SrRuO_3$ / (110) $SrTiO_3$ viewed along the $[001]_{SrTiO_3}$ zone axis. (a) and (b) are taken from the same sample shown in Fig. 5, showing (a) an OPB, (b) an atomically-clean twin boundary, and (c) the interface between $SrBi_2Nb_2O_9$ and the underlying faceted $SrRuO_3$ bottom electrode.

MICROSTRUCTURE OF FILMS GROWN ON (111) $SrTiO_3$

A cross-sectional high-resolution TEM image of a $SrBi_2Nb_2O_9$ film grown on (111) $SrTiO_3$ with an epitaxial $SrRuO_3$ bottom electrode is shown in Fig. 7. The *c*–axis in these films is tilted 56.6° away from the substrate surface normal, with the (103) $SrBi_2Nb_2O_9$ plane parallel to the surface of the substrate. As expected, this large tilt results in very high polarizations:

$P_r = 15.7$ □C/cm^2.[10] A high density of OPBs is observed in these films, and due to the large tilt many OPBs penetrate the full film thickness.

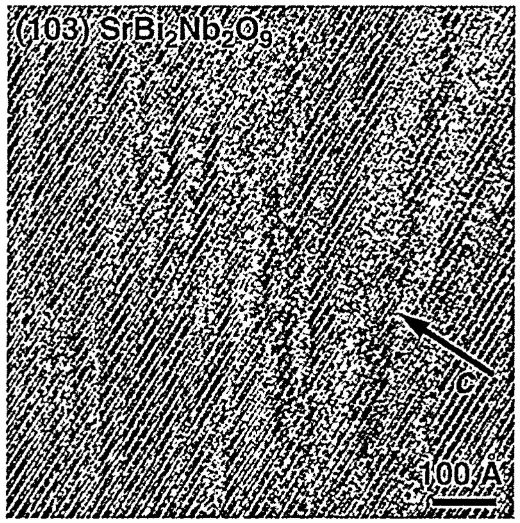

FIGURE 7 Cross-sectional high-resolution TEM image of a piece of the same (103) $SrBi_2Nb_2O_9$ / $(111)_{subcell}$ $SrRuO_3$ / (111) $SrTiO_3$ sample used for electrical characterization, viewed along the $[1\bar{1}0]_{SrTiO_3}$ zone axis. A high density of OPBs penetrating the full thickness of the film is apparent.

Figure 8 shows high-resolution TEM images of two views of twin boundaries in the same film: (a) a vertical twin boundary between two columnar grains in a cross-sectional image and (b) the meeting of the three twin variants in a plan-view image. The two grains in the cross-sectional view are equivalently oriented with respect to the substrate, but are viewed down different zone axes in the image due to the 120° rotational twinning. Twin boundaries observed in both orientations are free of second phases. Integral multiples of half unit-cell steps, due to the growth of the film in charge-neutral formula units, are visible in both views.

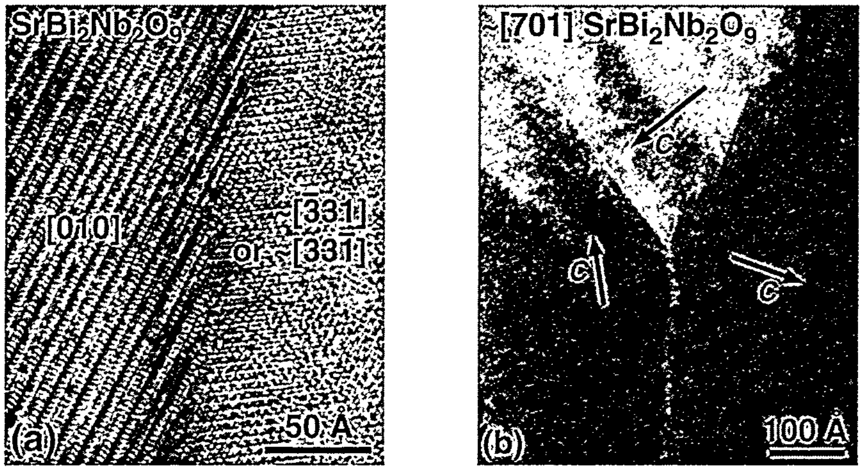

FIGURE 8 High-resolution TEM images of twin boundaries of the same (103) $SrBi_2Nb_2O_9$ / $(111)_{subcell}$ $SrRuO_3$ / (111) $SrTiO_3$ sample shown in Fig. 7: (a) in cross-section ($[1\bar{1}0]_{SrTiO_3}$ zone axis) showing the boundary between the two equivalently-tilted twins, and (b) in plan-view ($[111]_{SrTiO_3}$ zone axis) showing the intersection of three equivalently-tilted twinned grains. Twin boundaries viewed in both directions are observed to be free of second phases.

ACKNOWLEDGEMENTS

We gratefully acknowledge the financial support of the U.S. Department of Energy through grant DE-FG02-97ER45638 for the work performed at Penn State (PSU) and contract W-31-109-ENG-38 for the work performed at Argonne National Laboratory (ANL). In addition, we acknowledge the ANL Electron Microscopy Center (EMC), the University of Michigan at Ann Arbor Electron Microbeam Analysis Laboratory (EMAL), and the Pennsylvania State University Materials Characterization Laboratory (MCL) for use of their microscopy facilities.

REFERENCES

[1] C. A-Paz de Araujo, J. D. Cuchiaro, L. D. McMillan, M. C. Scott, and J. F. Scott, Nature **374**, 627 (1995).

[2] J. Lettieri, M. A. Zurbuchen, G. W. Brown, Y. Jia, W. Tian, X. Q. Pan, M. E. Hawley, and D. G. Schlom, Multicomponent Oxide Films for Electronics edited by M. E. Hawley, D. H. A. Blank, C. B. Eom, D. G. Schlom, and S. K. Streiffer, v. **574**, pp 31-36 (Materials Research Society, Pittsburgh, 1999).

[3] J. Lettieri, Y. Jia, M. Urbanik, C. I. Weber, J-P. Maria, D. G. Schlom, H. Li, R. Ramesh, R. Uecker, and P. Reiche, Appl. Phys. Lett. **73**, 2923 (1998).

[4] A. D. Rae, J. G. Thompson, R. L. Withers, and A. C. Willis, Acta Crystallogr., Sec. B **B46**, 474 (1990).

[5] A. D. Rae, J. G. Thompson, and R. L. Withers, Acta Crystallogr., Sec. B **B48**, 418 (1992).

[6] R. E. Newnham, R. W. Wolfe, and J. F. Dorrian, Mater. Res. Bull. **6**, 1029 (1971).

[7] K. Watanabe, M. Tanaka, E. Sumitomo, K. Katori, H. Yagi, and J. F. Scott, Appl. Phys. Lett. **73**, 126 (1998).

[8] M. A. Zurbuchen, J. Lettieri, Y. Jia, S. K. Streiffer, and D. G. Schlom, *submitted to* J. Mater. Res. (2000).

[9] J. Lettieri and D. G. Schlom *unpublished.*

[10] J. Lettieri, M. A. Zurbuchen, Y. Jia, D. G. Schlom, S. K. Streiffer, and M. E. Hawley, *to be published in* Appl. Phys. Lett. (2000).

[11] J. Lettieri, M. A. Zurbuchen, Y. Jia, D. G. Schlom, S. K. Streiffer, and M. E. Hawley, *submitted to* Appl. Phys. Lett. (2000).

[12] J. Lettieri, Y. Jia, S. J. Fulk, D. G. Schlom, M. E. Hawley, and G. W. Brown, *submitted to* Thin Solid Films (2000).

[13] M. A. Zurbuchen, J. Lettieri, Y. Jia, S. K. Streiffer, and D. G. Schlom, *to be submitted to* J. Mater. Res. (2000).

[14] M. A. Zurbuchen, J. Lettieri, Y. Jia, S. K. Streiffer, and D. G. Schlom, *to be submitted to* Appl. Phys. Lett. (2000).

[15] We have measured the polarization versus electric field for a *c*–axis oriented film of $SrBi_2Ta_2O_9$. It had no remanent polarization, confirming that no ferroelectric polarization occurs along the *c*–axis.